



## **Treatment of the surface water by Electrocoagulation-Electroflotation process in internal loop airlift reactor: Conductivity effect on turbidity removal and energy consumption**

**B. Bejjany<sup>1\*</sup>, B. Lekhlif<sup>2</sup>, F. Eddaqaq<sup>1,2</sup>, A. Dani<sup>1</sup>, H. Mellouk<sup>1</sup>, K. Digua<sup>1</sup>**

<sup>1</sup>*Laboratoire de Génie des Procédés et Environnement, FST Mohammedia, Université Hassan II Casablanca, Hay Yasmine, B.P. 146 Mohammedia, 20650, Maroc*

<sup>2</sup>*Equipe de recherche « Hydrogéologie, Traitement et Epuration des Eaux et Changements Climatiques », Ecole Hassania des Travaux Publics, Km 7, Route d'El Jadida, B.P 8108, Oasis, Casablanca, Maroc*

Received 1 Feb 2017,  
Revised 12Apr 2017,  
Accepted 14 Apr 2017

### **Keywords**

- ✓ Electrocoagulation,
- ✓ Electroflotation,
- ✓ Airlift reactor,
- ✓ turbidity,
- ✓ Energy consumption,
- ✓ surface water,
- ✓ Aluminum electrode.

*bejjany.bouchra@gmail.co  
m*

### **Abstract**

The aim of this paper is the potabilisation of surface water by an electrocoagulation-electroflotation process in internal loop Airlift reactor. The initial turbidity of the water to be treated is fixed at 107 NTU, a value generally found in surface waters. The tests were performed in airlift reactor of rectangular shape with an internal loop with a useful volume of 850 mL. The evaluation of the performance of the treatment is carried out by measuring, during the electrolysis time, the effect of the initial electrical conductivity on the reduction of the turbidity and the electrical energy consumption. During the treatment, three stages are distinguished: lag, reaction, and stable. In the reaction step, the electrocoagulation-electroflotation kinetics is rapid and it increases with the increase of the initial electrical conductivity of the solution  $\sigma_0$ . The processing time depends on the duration of the reaction step which decreases as  $\sigma_0$  increases. To achieve a turbidity abatement of 40%, the electrolysis time required for an initial conductivity solution  $\sigma_0$  of  $106 \mu\text{S} \cdot \text{cm}^{-1}$  is approximately 2.5 times the time for a solution of  $\sigma_0$  equal to  $351 \mu\text{S} \cdot \text{cm}^{-1}$ . This also applies to a reduction of 70% and 87%. As for energy consumption, it increases by about 30%. A correlation has been established, between the electrical energy consumed per  $\text{m}^3$  with the initial conductivity of the solution and the electrolysis time.

## **1. Introduction**

Surface waters intended for the production of drinking water contain many undesirable agents (suspended matter, bacteria, viruses, organic matter, etc.), making the use of water unfit for human consumption. These waters must be treated to comply with drinking water standards. The surface water treatment chain comprises several processes: pre-chlorination, coagulation-flocculation, decantation, filtration, etc... The suspended material composed of very small particle sizes whose colloidal particles are difficult to eliminate by simple decanting. Its stability results from a balance between the electrostatic forces of interparticle repulsion and the forces of attraction of Van-der Waals, resulting in a potential called zeta ( $\zeta$ ) negative. This potential can be annihilated by cations such as  $\text{Ca}^{2+}$ ,  $\text{Al}^{3+}$ ,  $\text{Fe}^{3+}$  during coagulation or electrocoagulation, which increases the probability of agglomeration of the fine particles to form larger flocs.

Electrocoagulation is used for the treatment of aqueous effluents from the textile industry [1], refineries [2], water containing heavy metals and metal trace elements (MTE) such as fluorine, arsenic, nickel as well as chromium (VI) [3-5], as well as surface waters [6-10]. This method consists in electrochemically dissolving a metal (anode) for the in situ production of a cationic coagulant. This reduces the zeta potential of the suspension, and therefore increases the probability of agglomeration of the fine particles to form larger flocs. Iron and aluminum are generally the most widely used metals. In addition to the electrochemical dissolution of the anode, called the sacrificial electrode, the electrodes (anode and cathode) undergo a chemical dissolution

which depends on the pH of the solution. It is elevated in an alkaline and acidic medium while it is low in neutral medium [11].

This electrochemical process can be carried out in a horizontal or vertical reactor and can operate continuously or discontinuously [12]. Several researchers have used magnetic stirrer as a mechanical agitator to promote contact between the coagulant and the elements to be removed in the water [4, 13-16]. Essadki et al. (2009) [17] and Lekhlif et al. (2013) [9] used, for their part, blade-type agitation drives. During the last decade, the application of Airlift external-loop reactors has developed in the field of electrocoagulation water treatment [3, 17-19]. The agitation of the reaction medium in this type of device is ensured by the rise of the bubbles in one of the two compartments of the reactor. Indeed, during the electrolysis, gas bubbles released in the vicinity of the electrodes create a recirculation of the clay suspension between the two compartments of the reactor (riser and downcomer), which replaces mechanical agitation.

In this work, the elimination of the turbidity of synthetic water containing clay and colloidal matter has been studied for potabilization. The method used is electrocoagulation-electroflotation in an inner-loop airlift, with aluminum-based planar electrodes. According to the literature [20-23], the main mechanisms responsible for the elimination of turbidity by electrocoagulation-electroflotation are formation of metal ions, neutralization of particles, agglomeration of the clay particles, production of solid aluminum hydroxides and flotation and / or decantation of the flocs.

The evaluation of the performance of the process studied is carried out by temporally monitoring parameters such as: current intensity, pH, conductivity, and turbidity of the clay suspension. Integration of the operating cost of the electrocoagulation process is necessary for the design of the treatment units, but this aspect is often overlooked in most studies. According to Donini et al. (1994) [24], 20% of the operating cost is due to the energy consumption and 80% to the quantity of dissolved aluminum for the treatment of a suspension of bentonite and kaolinite with a NaCl concentration between 0, 02 and 0.1 (% by mass). The same study reports that the energy cost becomes equivalent to the cost of aluminum when the passivation of the electrodes is important. In this study, the minimum cost of treatment of the aqueous suspension is determined.

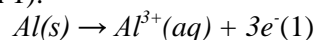
#### *Electrocoagulation mechanisms*

Electrocoagulation consists in placing two metal electrodes under a direct voltage, which causes an electro-dissolution of the anode. The ions thus formed constitute the coagulant necessary for the trapping of the pollutants. The metals commonly used are of flat shape [1] or of cylindrical shape [15]. The mounting of the electrodes can be monopolar [25] or bipolar [26].

The main reactions occurring at the terminals of the aluminum electrodes are:

#### *At the anode:*

Electro-dissolution of the anode leads to the release of the soluble  $\text{Al}^{3+}$  cations in the clay suspension according to the mechanism of the reaction (equation 1).



The  $\text{Al}^{3+}$  ions thus produced undergo spontaneous hydrolysis reactions leading to the formation of several monomeric species as  $\text{Al}(\text{OH})_3$ , and optionally its polymers, are coagulants which, in a pH range between 4 and 9.

Other reactions, called secondary reactions, may take place at the anode, particularly the generation of oxygen when the anodic potential is high [6].

#### *At the cathode:*

The water reduction reaction occurs, which results in the generation of hydrogen bubbles on its surface (equation 2):



These bubbles have a diameter of the order of 100  $\mu\text{m}$  and are originally the transport of the flocs formed towards the free surface (flootation process).

In addition to the oxidation and water reduction reactions, the anode and the cathode undergo chemical dissolution due to the attack of hydroxyl ions  $\text{OH}^{-}$  [16, 24].

## 2. Materials and methods

### 2.1. Preparation of synthetic solutions

Aqueous synthetic solutions were prepared from distilled water to which clay soil was added. The clay is screened to remove debris and coarse material from a screen with a mesh size of 45 µm. The sieve is then steamed for 3 hours. The solutions to be treated are prepared shortly before the electrocoagulation tests.

In a tank, two liters of distilled water and a quantity of pretreated clay are stirred. To approach the characteristics of surface water, the mixture is decanted to recover a suspension containing only colloids and clay particles smaller than 2 µm in size. The pre-clarifier used (Figure 1) is a height of 25.7 cm and an internal diameter of 19.4 cm.

The suspensions prepared are much diluted, so it is possible to study the rate of fall of an isolated spherical particle by applying the law of Stokes. Any calculation made, a particle with an apparent diameter of 2 µm would take 181 min to drop by 3.90 cm at a speed of 3.59 µm s<sup>-1</sup>. An overflow was installed at a distance of 3.90 cm from the free surface to recover the supernatant ( $H_{c2}-H_{c1} = 3.9$  cm). The diluted suspension constitutes the synthetic solution assimilated to surface water.

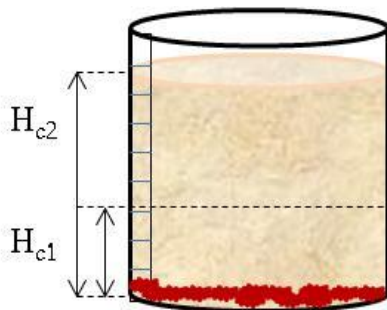


**Figure 1:** Clarifier unit for pre-treatment of the initial suspension

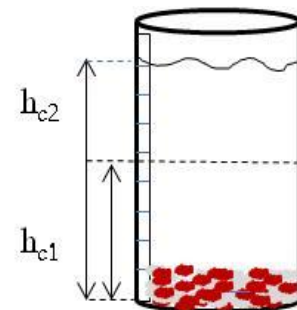


**Figure 2:** Clarifier unit of the suspension treated by electrocoagulation-electroflootation

The initial turbidity of the suspensions is adjusted to around 107 NTU. Three conductivities were selected 106, 232 and 351 µS.cm<sup>-1</sup>. This is adjusted by adding city water to the aqueous clay suspensions.

### 2.2. Sampling and analysis

At the beginning and end of each electrocoagulation test the pH, conductivity, turbidity and temperature of each solution are measured. The evolution of the current intensity was monitored throughout each electrocoagulation experiment. pH was measured using the Radiometer Analytical pH Meter / Ionomer PHM240, MeterLab® range. pH measuring ranges: -9 to +23 ± 0.002 pH, and a resolution of 0.001. The conductivity measurement was carried out using a HANNA HI 8733 portable conductivity meter. The conductivity meter is equipped with an integrated temperature sensor for automatic temperature compensation. The measuring range of the conductivity meter is from 0 to 1999 µS.cm<sup>-1</sup> ± 1% full scale, and a resolution of 1 µS.cm<sup>-1</sup>. Turbidity was measured using a HACH 2100N Turbidimeter measuring range from 0 to 1000 NTU ± 2% with a resolution of 0.001 NTU.

### 2.3. Experimental apparatus

The electrocoagulation tests were carried out in a rectangular airlift internal loop reactor schematically shown in FIG. 3. The reactor dimensions were as follows: capacity: 850 mL; Working height (a): 36 cm; Width (b): 5 cm; Height of injection zone (c): 4 cm and Height recirculation zone (d): 2.3 cm. Flat aluminum bars are used as electrodes, with a total height of 50 cm, a thickness of 0.2 cm and a width of 2.5 cm. The surface of the anode is 90 cm<sup>2</sup>, and the inter-electrode distance is maintained at 1.8 cm during all electrocoagulation tests. The latter are totally immersed in the Riser, and subjected to a voltage of 12 V thanks to a DC voltage generator.

The monitoring of the reduction in turbidity for different reaction times made it possible to measure the removal efficiency of the clay suspension by electrocoagulation and electroflootation. The experiments were carried out in time intervals ranging from 2.5 to 25 min. The contents of the reactor were emptied at the end of each experiment, from below into a cylindrical clarifier (Figure 2) with a height of 18.5 cm and an internal diameter of 9.6 cm. A calculated sedimentation time corresponding to 15 min makes it possible to eliminate only the coarse particles with an apparent diameter greater than 2 µm. The recovery of the supernatant is carried out via an overflow located at 2.80 cm from the free surface ( $h_{c2}-h_{c1} = 2.8$  cm).

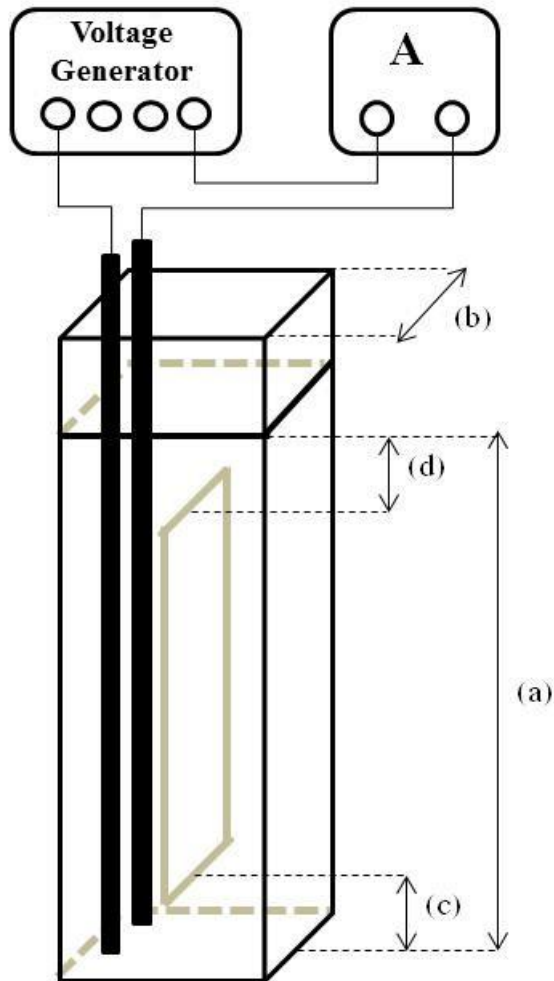


**Figure 3:** Schematic of laboratory-scale electrolytic airlift reactor system

#### 2.4. Determination of the consumed electrical energy ( $W_c$ )

The monitoring of the time evolution of the current intensity makes it possible to determine the consumed electrical energy  $W_c$  (Equation 3) for the treatment of water by the electrocoagulation-electroflotation process for the operating conditions used.

$$W_c \left( Wh / m^3 \right) = \frac{1}{V_R} \int_0^{\tau_e} U(t) I(t) dt \quad (3)$$

Where,

$W_c$ : the electrical power consumed per unit volume ( $Wh.m^{-3}$ ),

$U$ : the applied voltage (V),

$I$ : the intensity measured current (A),

$V_R$ : the volume of the reactor ( $m^3$ ),

$\tau_e$ : the electrolysis time (h).

In this study, the applied voltage  $U$  is constant and therefore the equation (3) becomes:

$$W_c \left( Wh / m^3 \right) = \frac{U}{V_R} \int_0^{\tau_e} I(t) dt \quad (4)$$

### 3. Results and discussion

#### 3.1. Electrocoagulation of synthetic ground water

During the first minutes of the starting of the electrolysis, two phenomena are observed at the anode. The first is the formation of a clear transparent strip at the anode / solution interface. The second is the concentration of small brown flocs separated from the electrode by the transparent layer. According to the literature, the zone of

transparency is called the boundary layer whose thickness is almost identical throughout the anode. This disappears at a few centimeters from the free surface where we observe the formation of foam. The boundary layer should result from the low bubble production at the electrodes due to the low conductivity of the solution, as noted in the test with the initial conductivity of  $106 \mu\text{S.cm}^{-1}$ . The predominant mode of transport is diffuse due to the low flow in the reactor. It disappears in tests where the conductivities are high, inducing a flow of convective type in the vicinity of the electrodes, more importantly due to the bubbles generated massively at the level of the electrodes.

On the other hand, the increase in electrical conductivity accelerates the recirculation of the bubbles between the two riser and downcomer compartments. This promotes more contacts between the small flocs and subsequently their agglomeration. This recirculation is not very perceptible at the start of the electrocoagulation process for the test with the initial conductivity  $\sigma_0 = 106 \mu\text{S.cm}^{-1}$ , contrary to the test with the initial conductivity  $\sigma_0 = 351 \mu\text{S.cm}^{-1}$ .

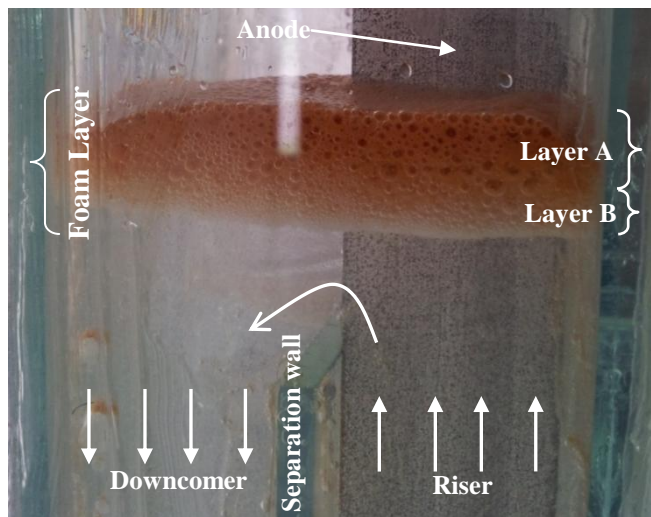


**Figure 4 :** view of the electrocoagulation treatment in the internal loop airlift reactor. Initial turbidity = 107 NTU ;  $U = 12 \text{ V}$  ;  $\sigma_0 = 351 \mu\text{S.cm}^{-1}$ ;  $\text{pH}_0=7,5$  ;  $\tau_e=20 \text{ min}$ .

Moreover, the upward movement of the bubbles produced at the electrodes drives the flocs towards the free surface of the reactor thus reducing the turbidity of the suspension and making the solid-liquid separation possible, as shown in Figure 4. The foam thus produced has a thickness, an appearance and therefore a composition which depends on several parameters: the processing time, the initial conductivity, the pH, the applied voltage and the inter-electrode distance. Initially, it is of whitish color and it takes very quickly the color of the clay (ocher-brown). This layer, easily separated from the water by scraping, contains gas bubbles, clay, colloidal material, aluminum hydroxides and possibly water-soluble impurities. For high operating times, a layer of whitish foam (layer A, Figure 4) is observed below the electrofloated layer (layer B, Figure 4). It should correspond to aluminum hydroxide. The overall thickness of the layer of foam formed on the free surface increases with electrolysis time and it reaches 14 mm for a time  $\tau_e = 20 \text{ min}$  and a conductivity  $\sigma_0 = 351 \mu\text{S.cm}^{-1}$ . There are also flocs which remain in suspension in the reactor and a very small amount of the decanted flocs in the reactor.

The pH of the solution, whatever the initial conductivity, varies little during electrolysis, as shown in Figure 5. It is the result of several reactions occurring in the synthetic solution: hydrolysis reaction of  $\text{Al}^{3+}$ , formation of hypochlorous acid from chlorine (existing in municipal water) reduced to the anode (equations 5, 6 and 7), etching of the electrodes by the  $\text{Cl}^-$  and  $\text{OH}^-$  ions and formation of the ions  $\text{OH}^-$  to the cathode. In the case of solutions having the conductivities of 232 and  $351 \mu\text{S.cm}^{-1}$ , it increases. This is probably due to the large formation of  $\text{OH}^-$  ions at the cathode or to an alkalization of the medium following a chemical dissolution of the cathode [20]. For the conductivity solution equal to  $106 \mu\text{S.cm}^{-1}$ , it appears that the decrease in pH is due to the hydrolysis and the formation of the hypochlorous acid.



Conductivity of the solution decreases little during electrolysis for all three tests. For the solution of initial conductivity  $\sigma_0 = 351 \mu\text{S} \cdot \text{cm}^{-1}$ , a decrease in the conductivity over time of the electrolysis is observed and it reaches 12% at  $\tau_e = 25$  min. For  $\sigma_0 = 106 \mu\text{S} \cdot \text{cm}^{-1}$  and  $\sigma_0 = 232 \mu\text{S} \cdot \text{cm}^{-1}$ , an increase in conductivity at  $\tau_e \leq 5$  min of 14% and 3%, respectively, followed by a decrease of no more than 7,4% to  $\tau_e > 5$  min.

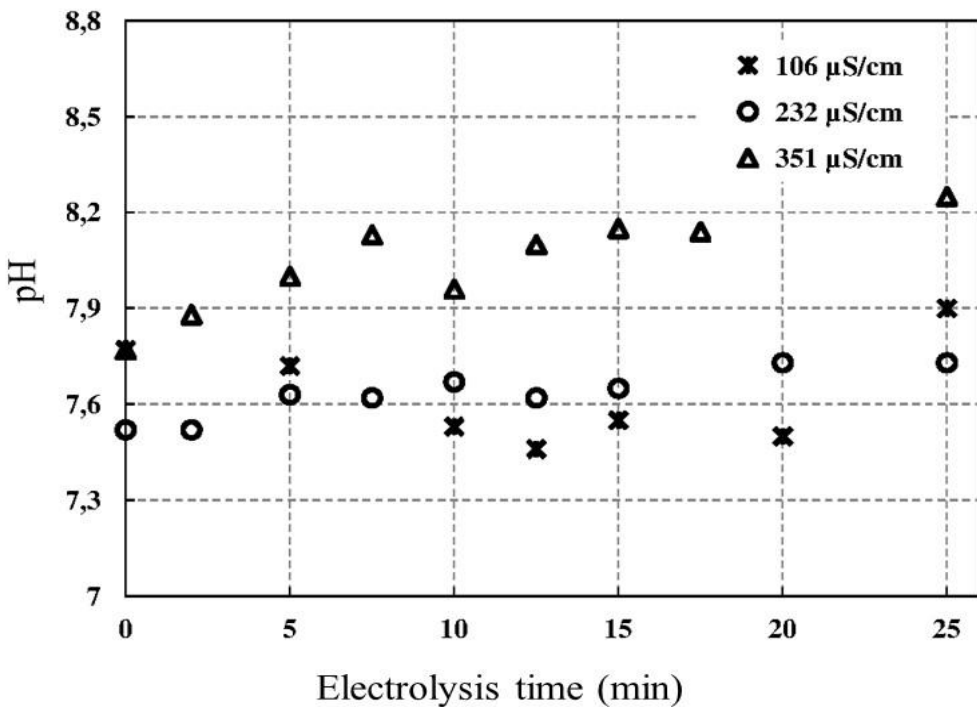


**Figure 5:** Temporal evolution of the pH for three initial conductivities of the solution ( $\sigma_0 = 106, 232$  and  $351 \mu\text{S} \cdot \text{cm}^{-1}$ ).

The decrease in conductivity can be attributed to the reduction of chloride ions by formation of chlorinated solid compounds, such as  $\text{Al}_{45}\text{O}_{45}(\text{OH})_{45}\text{Cl}$  as shown by Zidane et al. (2008) [27] or by anodic oxidation in the form of  $\text{Cl}_2$  [28], part of which reacts with water according to equations 5, 6 and 7.

Figure 6 shows the temporal evolution of the turbidity for different initial conductivities of the solution to be treated ( $\sigma_0 = 106, 232$  and  $351 \mu\text{S} \cdot \text{cm}^{-1}$ ). The appearance of the figure suggests three steps of elimination of turbidity by the electrocoagulation method described as follows:

1. Lag stage whose duration is noted  $\tau_{e1}$ , variable as a function of the initial conductivity: a slight increase in the turbidity of the solution is observed. For an initial conductivity of  $351 \mu\text{S} \cdot \text{cm}^{-1}$ , for example, a rise of 3% is recorded after an electrolysis time of 2 minutes ( $\tau_e = 2$  min). The time  $\tau_{e1}$  corresponds to the time when the turbidity is equal to the initial turbidity and it can be considered as the minimum time (lower limit) for the operation of the electrocoagulation-electroflocculation process. The increase in turbidity can be explained by the formation of aluminum hydroxide flocs, but with poor construction not allowing good contact with the clay particles. The reduction of the duration of the lag stage can be explained by the rapid dissolution of the anode releasing a significant amount of  $\text{Al}^{3+}$ .

2. Reaction stage, the duration of which is noted  $\tau_{e2}$ : elimination of the turbidity takes place rapidly, but depends on the conductivity of the medium, and it is almost linear in the case of a low initial conductivity of the solution ( $\sigma_0 = 106 \mu\text{S} \cdot \text{cm}^{-1}$ ). The slope therefore depends on the initial conductivity of the medium and becomes very high when this increases. In this step, the pH of the solutions studied is favorable to the formation of  $\text{Al}(\text{OH})_3$  which makes it possible to coagulate the colloidal particles by adsorption. During this step, there is formation of the visible flocs, a quantity of which is transported to the free surface by the fine bubbles generated in the vicinity of the surface of the electrodes. The elimination of the turbidity of the solution reaches the maximum at  $\tau_{e2}$ . The duration of this step ( $\tau_{e2} - \tau_{e1}$ ) depends on the conductivity and corresponds to the operating period of the electrocoagulation-electroflocculation process.

3. Stable (or neutral) stage: the turbidity abatement has reached its maximum. The residual concentration of the colloidal material reached 10 NTU. It cannot be further eliminated probably because of its low concentration or saturation of the adsorption sites on the aluminum hydroxide flocs. This step corresponds to the end of the

treatment and has to be controlled in order to avoid loss of electrical energy and any overconsumption of the electrodes which would cause contamination of the water and of the sludges produced by the excess of aluminum ions.

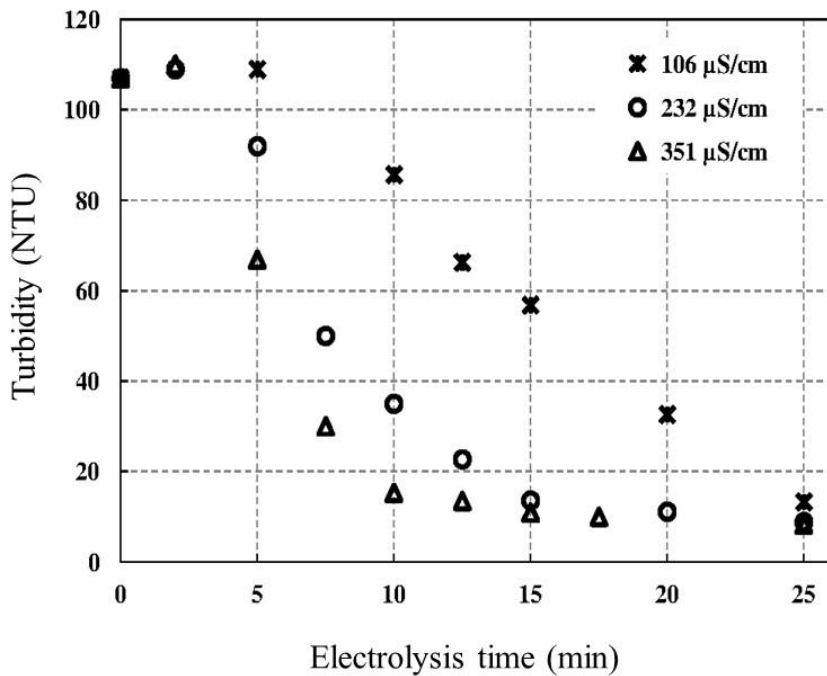


**Figure 6:** Temporal evolution of the turbidity for three initial conductivities of the solution ( $\sigma_0 = 106, 232$  and  $351 \mu\text{S}\cdot\text{cm}^{-1}$ ).

The duration  $\tau_{e1}$  is between 5 and 10 minutes for  $\sigma_0 = 106 \mu\text{S}\cdot\text{cm}^{-1}$ . This interval becomes tighter for  $\sigma_0 = 232 \mu\text{S}\cdot\text{cm}^{-1}$  and  $\sigma_0 = 351 \mu\text{S}\cdot\text{cm}^{-1}$  and evolves between 2 and 5 min. It would be detrimental to fix our operating time of the electrocoagulation process at values less than 2 minutes. To determine with precision the duration of the lag stage, it is necessary to make measurements at least every minute. The lag stage is a step of operation of the process where the dissolution of the anode begins to take place and the concentration of aluminum ions increases in the solution. During this period, the turbidity increases and the agglomeration of the particles is minimal. Elsayed et al. (2013) [25] showed that the clay removal efficiency is more than 75% for an electrolysis time of 2 minutes with a pH of 10.52, a NaCl concentration of 1 g.L<sup>-1</sup> and a density of Current between 10.13 and 29.1 A.cm<sup>-2</sup>. With the operating conditions of Elsayed et al. (2013) [25],  $\tau_e = 2$  min is greater than the duration of the lag stage of the operation of the method. Reduction in the duration of the lag stage is explained by rapid electrochemical dissolution of the anode to release a significant amount of Al<sup>3+</sup> in the solution which destabilizes the clay particles by reducing the zeta potential and hence facilitates coagulation. Indeed, the mechanical stirring extracts the material from the vicinity of the electrodes and accelerates the coagulation, which could explain the absence of the lag stage. It should also be noted that the duration of the lag stage decreases with the increase of the initial conductivity.

The duration of the reaction step of the electrocoagulation-electroflootation process depends on the initial conductivity  $\sigma_0$ :

- $\tau_{e2} = 25$  min for  $\sigma_0 = 106 \mu\text{S}\cdot\text{cm}^{-1}$ . The duration of this step exceeds 15 minutes and less than 20 minutes ( $15 < \tau_{e2} - \tau_{e1} < 20$ ).
- $\tau_{e2} = 15$  min for  $\sigma_0 = 232 \mu\text{S}\cdot\text{cm}^{-1}$ . The duration of the reaction step exceeds 10 minutes and less than 13 minutes ( $10 < \tau_{e2} - \tau_{e1} < 13$ ).
- $\tau_{e2} = 10$  min for  $\sigma_0 = 351 \mu\text{S}\cdot\text{cm}^{-1}$ . The duration of the reaction step exceeds 5 minutes and less than 8 minutes ( $5 < \tau_{e2} - \tau_{e1} < 8$ ).

During the reaction which lasts ( $\tau_{e2} - \tau_{e1}$ ), there is formation of the visible flocs, a large quantity of which is transported to the free surface by the fine bubbles generated in the vicinity of the surface of the electrodes. The elimination of the turbidity of the solution reaches the maximum at  $\tau_{e2}$  which depends on the initial conductivity of the solution.

Holt et al. (2002, 2005) [14, 29] indicated the same trend (three operating stages) for the removal of clay or colloidal matter by the electrocoagulation process. Rahmani (2008) [8], Kilic and Hosten (2010) [30] and

Elsayed et al. (2013) [25] did not, in turn, observe the lag stage of operation of the process. Some authors observed only the stabilising stage [31]. This can be explained by the short duration of the reaction stage and turbidity as well as the time chosen to carry out the analyses. The duration of these stages being closely related to the operating conditions.

### 3.2. Amount of aluminum consumed

Under the same operating conditions and for the same applied voltage, increasing the conductivity of the solution leads to an increase in the current density. This is accompanied by an increase in the amount of aluminum dissolved as  $\text{Al}^{3+}$  in the solution. This quantity can be quantified using the Faraday law (equation 13) which makes it possible to estimate the theoretical mass  $m_{th}$  of the electrochemically dissolved aluminum.

$$m_{th}(g) = \frac{M}{n_e F} \int_0^{\tau_e} I(t) dt \quad (8)$$

Where,

$\tau_e$  is the electrolysis time (s),

M is the molar mass of aluminum ( $M = 27 \text{ g.mol}^{-1}$ ),

$n_e$  is the number of electrons released by electro-oxidation of the aluminum anode ( $n_e = 3$ ),

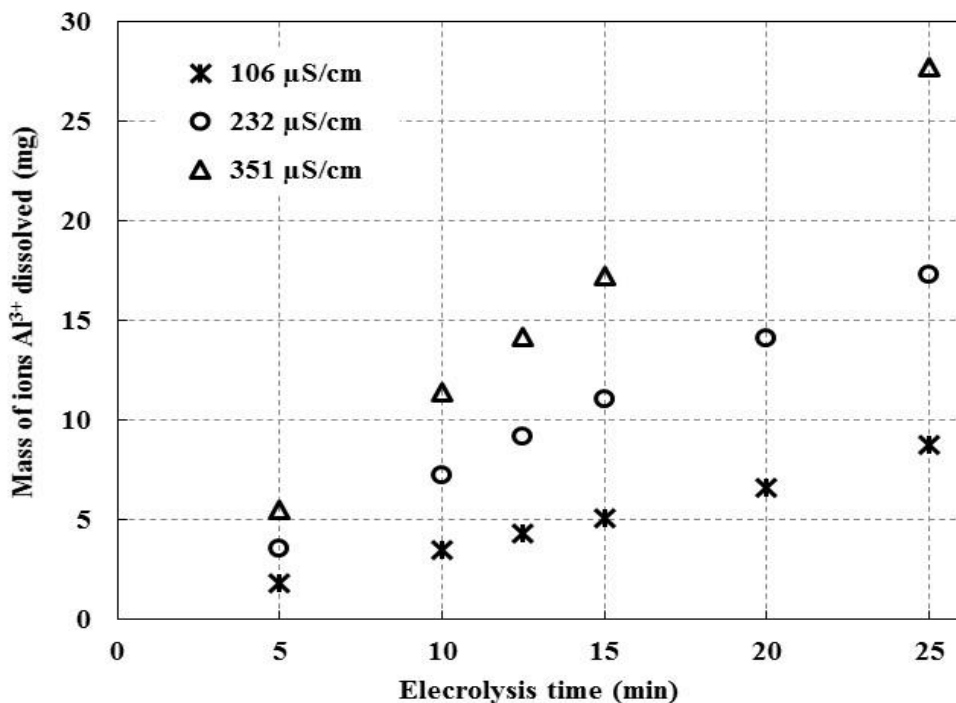
F is the Faraday constant ( $F = 96500 \text{ C.mol}^{-1}$ ).

In this study, the theoretical mass of aluminum can be expressed as a function of the energy consumed per unit volume  $W_c$  and equation (13) becomes:

$$m_{th}(g) = \frac{1}{3600} \frac{M}{n_e F} \frac{V_R}{U} W_c (\text{Wh.m}^{-3}) \quad (9)$$

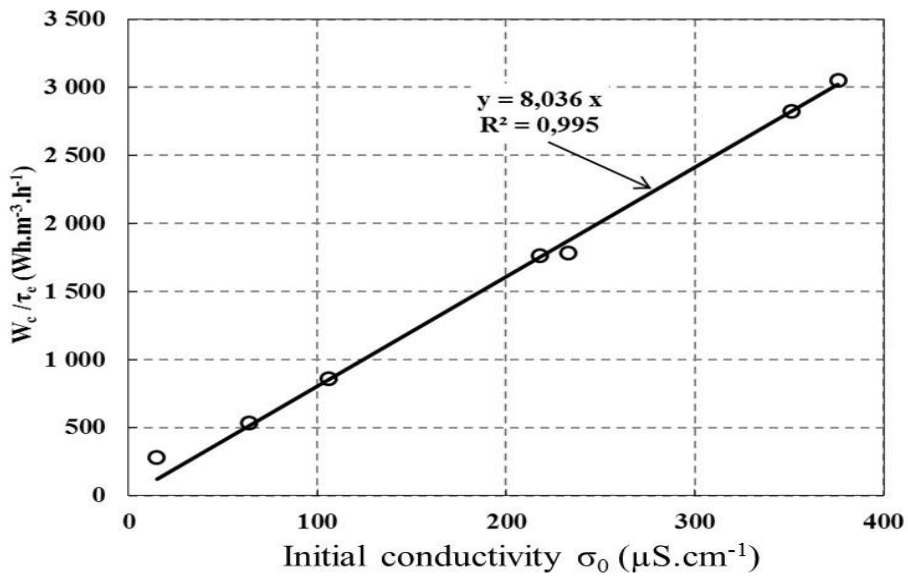
According to equation 9, the quantity of electro-dissolved aluminum is proportional to the energy consumed per unit volume ( $W_c$ ), which depends on the applied potential, the inter-electrode distance, the useful area of the electrodes, the conductivity of the solution and the degree of passivation of the cathode.

Figure 7 summarizes the masses of aluminum dissolved according to Faraday's law for the three initial conductivities of the solutions to be treated ( $\sigma_0 = 106, 232, 351 \mu\text{S.cm}^{-1}$ ).



**Figure 7:** Mass of ions  $\text{Al}^{3+}$  dissolved (in mg) according to the Faraday law for three initial conductivities ( $\sigma_0 = 106, 232, 351 \mu\text{S.cm}^{-1}$ ).  $U=12 \text{ V}$ ,  $d_{\text{inter}}=1.8 \text{ cm}$  et  $S_a=90 \text{ cm}^2$

It is found that the amount of dissolved aluminum increases as a function of the electrolysis time for a given initial conductivity of the solution and for the same time of electrolysis, it increases with the increase of the initial conductivity of the solution.



**Figure 8 :** Effect of the initial conductivity on energy consumption per  $\text{m}^3$  divided by divided by the electrolysis time.

The energy consumption per unit of time increases linearly with the initial conductivity of the solution to be treated and varies linearly with the electrolysis time for a solution to be treated with given initial conductivity as shown in Figure 8. On the basis of the experimental results, a correlation between energy consumption, initial conductivity and electrolysis time was established (equation 10).

$$W_c (\text{Wh}/\text{m}^3) = 8.036 \sigma_0 \tau_e \quad (2)$$

The constant 8.036 depends on the surface of the anode, the inter-electrode distance, and the voltage applied. This equation is therefore valid only for our operating conditions and the generalization of this relation requires the realization of a companion of measurements by varying the other parameters. As shown in Table 1, to achieve a removal efficiency of about 40%, the electrolysis time required for an initial conductivity solution of  $106 \mu\text{S} \cdot \text{cm}^{-1}$  is 2.5 times that required for a solution, and increase in energy consumption by 27.8%.

**Table1 :** comparison between electrolysis time and energy consumption for different turbidity removal efficiencies (about 40 %, 70 % et 87 %)

$\sigma_0$ ( $\mu\text{S}/\text{cm}$ )	E (%)	$\tau_e$ (min)	$W_c (10^{-3} \text{ kWh}/\text{m}^3)$	$m_{theo}(\text{mg})$	Minimum operating cost ( $\text{US } \$/\text{m}^3$ )
<i>Removal efficiency to about 38%</i>					
106	37.5	12.5	179.6	4.272	0.0320
351	38.0	5	229.9	5.468	0.0410
<i>Removal efficiency to about 70%</i>					
106	69.5	20	275.7	6.557	0.0492
232	67.3	10	304.7	7.247	0.0543
351	72.0	7,5	356.7	8.483	0.0636
<i>Removal efficiency to about 87 % (correspond à <math>\tau_e = \tau_{e2}</math>)</i>					
106	87.6	25	368.2	8.756	0.0657
232	87.3	15	464.3	11.041	0.0828
351	85.7	10	478.8	11.386	0.0854

It took an electrolysis time ratio of 2.66 to achieve a turbidity abatement of about 70% which was accompanied by an increase in energy consumption of 29.4%. It can be seen that for the two abatements, the ratio of the treatment time is about 2.5 and the energy consumption is about 30%.

Furthermore, to achieve a removal efficiency of approximately 70%, the electrolysis time required for an initial conductivity solution of  $106 \mu\text{S.cm}^{-1}$  is 2 times the time required for an initial conductivity solution of  $232 \mu\text{S.cm}^{-1}$ . On the contrary, energy consumption increases by about 10%.

From this analysis, it can be seen that the increase in conductivity is favorable in order to reduce the processing time. Contrary wise, it is a disadvantage for the energy consumption required for the electrochemical dissolution of the anode and consequently an increase in the operating cost.

### 3.3. Cost of treatment:

The efficiency of the current, which is the ratio between the mass actually dissolved during the electrolysis and the theoretical mass predicted by the Faraday law (equation 13), is a key parameter for evaluating the electrocoagulation- Electroflotation. In most cases, current efficiency exceeds 100% [13, 24]. However, the amount of aluminum involved in the electrocoagulation process is not only due to the electrochemical dissolution of the anode but also to a chemical dissolution of the electrodes.

$$E (\%) = \frac{m_{rel} (g)}{m_{th} (g)} \cdot 100 \quad (11)$$

This parameter should be taken into account when studying the cost of the operation. According to Donini et al., 1994 [24], 20% of the cost of the electrocoagulation process is due to electrical consumption and 80% is attributed to the amount of aluminum consumed when there is no passivation of the cathode.

**Table 2:** Low voltage tariffs - professional: customers driving force, industrial and agricultural (tariffs of 01/12/2016). Source: Official website of the ONEE Electricity Branch)

Monthly consumption ranges	Price of kWh (Morrocan dirham)	Price of kWh (US \$)
0 - 100 kWh	1.3179	0.130
101 - 500 kWh	1.4169	0.140
> 500 kWh	1.6193	0.160

Table 2 represents the price including the kWh low voltage tax for the industrial sector in Morocco. The minimum price of one kWh ( $P_{kWhMin}$ ) is US \$ 0.13 and the price per kilogram of aluminum (PAI) is around US \$ 1.7281 (US \$ 1.7281) Aluminum from 01/12/2016. This price of aluminium is the minimum because it does not take into account the transformations necessary to manufacture the electrodes in the form of plates.

The minimum operating cost per  $\text{m}^3$  ( $CF_{Min}$ ) for the treatment of surface water by the electrocoagulation-electroflotation process is the sum of the minimum cost of the electrical energy consumed and the quantity of electro-chemically dissolved aluminum (equation 12).

$$CF_{Min} (\$/\text{m}^3) = \frac{1}{V_R} m_{th} (\text{kg}) \times P_{Al} + W_c (\text{kWh}/\text{m}^3) \times P_{kWhMin} \quad (12)$$

For the treatment of one cubic meter of an initial turbidity suspension of 107 NTU, the minimum operating cost varies between 0.032 and 0.0854 \$ US ( $0.032 \leq CF_{Min} \leq 0.0854$ ) for varying treatment efficiencies between 38% and 87% (Table 1). Based on our experimental results, the energy cost represents about 73% of the minimum operating cost. By replacing the mass of electro-chemically dissolved aluminum by its expression (equation 9), the equation (12) becomes:

$$CF_{Min} (\$/m^3) = \left( \frac{0.000001}{3600} \frac{M}{n_e F} \frac{1}{U} P_{Al} + P_{kWhMin} \right) \times W_c (\text{kWh/m}^3)$$

## Conclusion

The electrocoagulation process associated with airlift has effectively eliminated the turbidity of synthetic solutions related to surface water, in particular by coupling electrocoagulation with electroflootation and by recirculation created by gas bubbles from the electrolysis process. These processes are accelerated as the conductivity of the synthetic solution increases. To achieve a yield of 90.6%, the solution with the conductivity of 106  $\mu\text{S}/\text{cm}$  requires a time of about 25 minutes, while for 232  $\mu\text{S}/\text{cm}$  and 351  $\mu\text{S}/\text{cm}$ , they require respectively 20 minutes and 15 minutes.

During the electrolysis time, three distinct steps are distinguished, the most important of which is that corresponding to the elimination of the turbidity. During this step, there is formation of the visible flocs, a quantity of which is transported to the free surface by the fine bubbles generated in the vicinity of the surface of the electrodes. The turbidity is removed by adsorption onto the aluminum hydroxide flocs at pH favorable to the formation of  $\text{Al(OH)}_3$ . In this step, the electrocoagulation-electroflootation kinetics is rapid and increases when the initial electrical conductivity of the solution increases. To achieve turbidity abatement efficiencies of 40% and 70%, the electrolysis time required for an initial conductivity solution  $\sigma_0$  of 106  $\mu\text{S}\cdot\text{cm}^{-1}$  is about 2.5 times the time required for a solution of  $\sigma_0$  is equal to 351  $\mu\text{S}\cdot\text{cm}^{-1}$ . On the contrary, energy consumption increases by about 30%. A correlation was established between the energy consumed per unit volume and the initial conductivity of the solution and the electrolysis time.

## References

1. Kobya M., Can O.T., Bayramoglu M., *J. Hazard. Mater.*, 100 (2003) 163-178.
2. Ben Hariz I., Halleb A., Adhoum N., Monser L., *Sep. Purif. Technol.*, 107 (2013) 150-157.
3. Bennajah M., Gourich B., Essadki A.H., Vial Ch., Delmas H., *Chem. Eng. J.*, 148 (2009) 122-131.
4. Kobya M., Ulu F., Gebologlu U., Demirbas E., Oncel M.S., *Sep. Purif. Technol.*, 77 (2011) 283-293.
5. Lekhlif B., Oudrhiri L., Zidane F., Drogui P., Blais J.F., *J. Mater. Environ. Sci.*, 5 (1) (1994) 111-120.
6. Cañizares P., Martinez F., Jiménez C., Lobato J., Rodrigo M.A., *Sep. Sci. Technol.*, 42 (2007) 2157-2175.
7. Cañizares P., Martinez F., Rodrigo M.A., Jiménez C., Saez C., Lobato J., *Sep. Purif. Technol.*, 60 (2008) 155-161.
8. Elsayed E.M., Zewail T.M., Zaatout A.A., *J Chem. Eng. Process Technol.*, 4 (9) (2013).
9. Lekhlif B., Eddaqaq F., Dani A., Digua K., Bejjany B., Lakhdar E., AitYacine Z., Hanine H., *Phys. Chem. News*, 69 (2013) 52-60.
10. Eddaqaq F., Lekhlif B., Dani A., Digua K., *SSRG Inter. J. App. Chem.*, 3 (5) (2016) 1-6.
11. Mokaddem M., Volovitch P., Rechou F., Oltra R., Ogle K., *Electrochim Acta*, 55 (2010) 3779-3786.
12. Chen G., *Sep. Purif. Technol.*, 38 (2004) 11-41.
13. Jiang J.Q., Graham N., André C., Kelsall G.H., Brandon N., *Water Res.*, 36 (2002) 4064-4078.
14. Holt P., Barton G., Mitchell C., *Chemosphere*, 59 (2005) 355-367.
15. Tezcan Un U., Savas Koparal A., Bakir Ogutveren U., *Chem. Eng. J.*, 223 (2013) 110-115.
16. Szynkarczuk J., Kan J., Hassan T. A. T., Donini J. C., *Clays Clay Miner.*, 42(6) (1994) 667-673.
17. Essadki A.H., Gourich B., Vial Ch., Delmas H., Bennajah M., *J. Hazard. Mater.*, 168 (2009) 1325-1333.
18. Balla W., Essadki A.H., Gouricha B., Dassaa A., Chenik H., Azzib M., *J. Hazard. Mater.*, 184 (2010) 710-716.
19. Essadki A.H., Gourich B., Vial H., Delmas Ch., *Chem. Eng. Sci.*, 66 (2011) 3125-3132.
20. Mouedhen G., Feki M., De PetrisWery M., Ayedi H.F., *J. Hazard. Mater.*, 150 (2008) 124-135.
21. MattesonM.J., Regina L. Dobson, Robert W., Glenn Jr., Nagesh S. Kukunoor, William H. Waits III, Eric J., *Clayfield, Colloids Surf. A*, 104 (1995) 101-109.

22. Amirtharajah A., *J. Am. Water Work Assoc.*, 80 (12) (1988) 36-46.
23. Lu S., Pugh R.J., Forssberg E., *Interfacial Separation of Particles*, Elsevier, Amsterdam 1<sup>st</sup> edition (2005), ISBN: 0-444-51606-9.
24. Donini J.C., Kan J., Szynkarczuk J., Hassan T.A.T., Kar K.L., *The Can. J. Chem. Eng.*, 72 (1994) 1007-1012.
25. Rahmani AR., *J. Res. Health Sci.*, 8 (2008) 18-24.
26. Malakootian M., Mansoorian, Moosazadeh M. H., *J. hardness from drinking water Desalination*, 255 (2010) 67-71.
27. Zidane F., Drogui P., Lekhlif B., Bensaid J., Blais J.F., Belcadi S., Kacemi K., *J. Hazard. Mater.*, 155 (2008) 153-163.
28. Abuzaid N.S., Bukhari A.A., Hamouz., *Adv. Environ. Res.*, 6 (2002) 325–333.
29. Holt P., Barton G., Wark M., Mitchell C., *Colloids Surf. A*, 211 (2002) 233-248.
30. Kılıç M., Hosten C., *J. Hazard. Mater.*, 176 (2010) 735-740.
31. Phalakornkule C., Worachai W., Satitayut T. Inter., *Schol. Sci. Res. Innov.*, 4 (2010) 233-239.

(2017) ; <http://www.jmaterenvironsci.com>